Scientific Research Publishing

Open Journal of Applied Sciences, 2023, 13, 2186-2197
https://www.scirp.org/journal/ojapps
ISSN Online: 2165-3925
ISSN Print: 2165-3917

Effects of Physical Parameters and Time-Delay Coefficients on the Amplitude and Frequency Bandwidth of Saturation Controller for a Beam Vibration

Qiqi Li, Yanying Zhao, Jiacai Zhou, Weikai Wang

School of Aircraft Engineering, Nanchang Hangkong University, Nanchang, China
Email: pom5i5@163.com

How to cite this paper: Li, Q.Q., Zhao, Y.Y., Zhou, J.C. and Wang, W.K. (2023) Effects of Physical Parameters and Time-Delay Coefficients on the Amplitude and Frequency Bandwidth of Saturation Controller for a Beam Vibration. *Open Journal of Applied Sciences*, **13**, 2186-2197.
https://doi.org/10.4236/ojapps.2023.1311170

Received: October 7, 2023
Accepted: November 26, 2023
Published: November 29, 2023

Abstract

In this paper, the influence of physical parameters on the width of saturated control frequency band and the influence of time delay parameters on the stability of saturated control system are studied. The analytical solution of the motion equation of the system when the main resonance and the 1:2 internal resonance occur simultaneously is obtained by multiple scale method, experimentally measured natural frequencies of nonlinear beams. The effects of excitation amplitude, delay feedback coefficients and nonlinear coefficients on saturation control are investigated. The results of the study show that the bandwidth of the saturation control can be increased by increasing the value of the external excitation, the nonlinear coefficients enhance the nonlinear phenomena of the system.

Keywords

Time-Delay, Nonlinear, Saturation Controller, Bandwidth

1. Introduction

In recent years, the theory and technique of vibration suppression have been studied extensively. In order to suppress the vibration of the main system, various controllers have been developed. The saturation phenomenon means that when the system is stimulated by the main resonance type, the amplitude of the main system response increases with the increase of the amplitude of the external excitation. When the amplitude of the external excitation exceeds a certain critical value, the amplitude of the main system response reaches saturation and

no longer increases, then the energy is transferred to the secondary system when the amplitude of the external excitation continues to increase. Saturation phenomenon was first discovered by Nayfeh *et al.* [1] when analyzing the coupling motion of pitch and roll of ships. Haddow *et al.* [2] proved the saturation phenomenon through experiments and proposed that the saturation phenomenon could be used to make shock absorbers. Golnaraghi [3] was the first to introduce internal resonance in nonlinear control to control the transient free-response vibration of a beam. Oueini *et al.* [4] studied a nonlinear controller based on saturation phenomenon as a vibration absorber for the linear model of a cantilever beam. Oueini and Golnaragi [5] proposed the use of a linear second-order analog electronic circuit controller coupled to a vibrational structure by a quadratic nonlinear term. Khajepour and Golnaraghi [6] then implemented the technique on a PZT mount-driven cantilever beam. Macarri [7] studied the vibration of the main resonance of a cantilever beam controlled by time-delay state feedback. Pai *et al.* [8] gave the analytical, numerical and experimental results of nonlinear saturation control and linear position feedback algorithms, introduced the advantages of hybrid, proportional linear and saturated nonlinear controllers, and then coupled the two algorithms and applied them to experimental tests. Xu *et al.* [9] discussed delayed saturation controller used to suppress the vibration of stainless steel beams, and studied the first-mode vibration of stainless-steel beam. Zhao and Xu [10] studied the suppression effect of delayed feedback on vertical displacement vibration in two-degree-of-freedom nonlinear dynamical systems. Zhao and Xu [11] studied delayed feedback control and saturation control to eliminate the vibration of the dynamic system.

For active control systems, the delay in control processing is caused by transmission delay, measurement of system state, online calculation, data filtering and processing, and the delay caused by the execution of control force. When the control system is applied to a mechanical or structural system, the time delay phenomenon is particularly common, which can limit the performance of the feedback controller. In many systems, the inevitable time delay in the controller will complicate the system behavior and may lead to instability of the dynamic system. Therefore, it is very important to consider the influence of time delay on the system vibration reduction characteristics in nonlinear saturation control vibration reduction systems. This paper mainly studies the influence of physical parameters and time delay parameters on the amplitude and frequency band width of nonlinear beam vibration saturation controller. The structure of this article is as follows. Firstly, the motion equation of the beam is given, and the perturbation analysis and stability analysis of the equilibrium solution are given respectively in Section 2. In Section 3, the natural frequency of the cantilever beam is measured, and in Section 4, the influence of physical parameters and delayed feedback control on the saturation control is studied. In nonlinear saturated control systems, when numerical simulation is carried out, it is found that the nonlinear system is more sensitive to the initial value, and a little change in the initial value leads to system instability, and the study of the time-delay coeffi-

cients and the physical parameters of the damping system of the bandwidth is particularly important, and at the same time, it also provides a theoretical basis for engineers and technicians to the real-time operation of the control system.

2. Equations of Motion with the Saturation Control

Warminski *et al.* [12] studied the application of saturation control in flexible geometric nonlinear beam-like structures with macro-fiber composite (MFC) actuators. Based on this model, the dynamic system model in this paper is coupled with two velocity delay feedback control variables, and the corresponding system differential equation is shown in the equation.

$$\begin{cases} \ddot{u}+2\zeta_1\omega_1\dot{u}+\omega_1^2u+\beta u^3-\delta\left(u\dot{u}^2+u^2\ddot{u}\right)=f\cos(\Omega t)+\gamma v^2\left(t-\tau_1\right)+g_1\dot{u}\left(t-\tau_4\right) \\ \ddot{v}+2\zeta_2\omega_2\dot{v}+\omega_2^2v=\alpha\dot{u}\left(t-\tau_2\right)v\left(t-\tau_3\right)+g_2\dot{v}\left(t-\tau_5\right) \end{cases} \tag{1}$$

where u, ω_1 and v, ω_2 are the displacements and the natural frequencies of the cantilever beam and controller respectively. ζ_1 and ζ_2 are the damping coefficients of the cantilever beam and controller respectively. β and δ are the system nonlinear coefficients respectively, while γ and α denote the quadratic nonlinear feedback gain coefficients respectively. f and Ω are the external excitation amplitude and frequency respectively. $g_1\dot{u}\left(t-\tau_4\right)$ and $g_2\dot{v}\left(t-\tau_5\right)$ are the velocity feedback signals of the cantilever beam and the saturation controller respectively, g_1 and g_2 are the feedback gain coefficients of the cantilever beam and the controller, τ_4 and τ_5 are the feedback time delays. $\gamma v^2\left(t-\tau_3\right)$ is feedback signal of the controller.

2.1. Mathematical Analysis

In order to analyze the nonlinear saturated system described above, introducing a formal small-scale parameter ε $(0<\varepsilon<1)$ to find the solution of steady states of Equation (1). It can be set that: $\zeta_1=\varepsilon\zeta_1$, $\zeta_2=\varepsilon\zeta_2$, $g_1=\varepsilon g_1$, $g_2=\varepsilon g_2$, $\beta=\varepsilon^{-1}\beta$, $\delta=\varepsilon^{-1}\delta$, $f=\varepsilon^2 f$. The method of multiple scales is employed to seek second order approximate solutions of (1), Then set the displacements of the cantilever beam and the controller u and v and the time-delay value v_{τ_1}, u_{τ_2}, v_{τ_3}, u_{τ_4}, v_{τ_5} are solved as follows:

$$u\left(t,\varepsilon\right)=\varepsilon u_1\left(T_0,T_1\right)+\varepsilon^2u_2\left(T_0,T_1\right)+\cdots \tag{2}$$

$$v\left(t,\varepsilon\right)=\varepsilon v_1\left(T_0,T_1\right)+\varepsilon^2v_2\left(T_0,T_1\right)+\cdots \tag{3}$$

$$v_{\tau_1}\left(t,\varepsilon\right)=\varepsilon v_{1\tau_1}\left(T_0,T_1\right)+\varepsilon^2v_{2\tau_1}\left(T_0,T_1\right)+\cdots \tag{4}$$

$$u_{\tau_2}\left(t,\varepsilon\right)=\varepsilon u_{1\tau_2}\left(T_0,T_1\right)+\varepsilon^2u_{2\tau_2}\left(T_0,T_1\right)+\cdots \tag{5}$$

$$v_{\tau_3}\left(t,\varepsilon\right)=\varepsilon v_{1\tau_3}\left(T_0,T_1\right)+\varepsilon^2v_{2\tau_3}\left(T_0,T_1\right)+\cdots \tag{6}$$

$$u_{\tau_4}\left(t,\varepsilon\right)=\varepsilon u_{1\tau_4}\left(T_0,T_1\right)+\varepsilon^2u_{2\tau_4}\left(T_0,T_1\right)+\cdots \tag{7}$$

$$v_{\tau_5}\left(t,\varepsilon\right)=\varepsilon v_{1\tau_5}\left(T_0,T_1\right)+\varepsilon^2v_{2\tau_5}\left(T_0,T_1\right)+\cdots \tag{8}$$

where $T_0 = t$ is the fast-varying time scale, $T_1 = \varepsilon t$ is the slow-varying time scale, and $T_n = \varepsilon^n t\left(n = 0,1,2,\cdots\right)$ is the newly introduced independent variable.

In the following, the system is analyzed in the presence of a 1:1 primary resonance and a 1:2 internal resonance, whose coefficients are required to be equal to zero, and convert small-divisors into secular terms by introducing the detuning parameters σ_s and σ_c according to:

$$\Omega = \omega_1 + \varepsilon\sigma_s, \quad 2\omega_2 = \omega_1 + \varepsilon\sigma_c \tag{9}$$

we can obtain the solvability conditions:

$$\begin{aligned} &-A_2^2\gamma \mathrm{e}^{i\sigma_c T_1 - 2i\tau_1\omega_2} + 3A_1^2\beta\overline{A_1} + 2A_1^2\delta\overline{A_1}\omega_1^2 + 2iA_1\zeta_1\omega_1^2 \\ &+ 2iA_1'\omega_1 - \frac{1}{2}f\mathrm{e}^{i\sigma_s T_1} + A_1 g_1 i\omega_1 \mathrm{e}^{-i\tau_4\omega_1} = 0 \end{aligned} \tag{10}$$

$$\alpha i\omega_1 A_1\overline{A_2}\mathrm{e}^{i\left(\tau_3\omega_2 - \tau_2\omega_1 - T_1\sigma_c\right)} - i\omega_2\left(2\zeta_2\omega_2 A_2 + 2A_2'\right) - A_2 g_2 i\omega_2 \mathrm{e}^{-i\tau_5\omega_2} = 0 \tag{11}$$

Introducing polar notation $A_1 = \frac{1}{2}a_1\left(T_1\right)\mathrm{e}^{i\theta_1\left(T_1\right)}$ and $A_2 = \frac{1}{2}a_2\left(T_1\right)\mathrm{e}^{i\theta_2\left(T_1\right)}$ into Equation (10) and Equation (11), then separating the real and imaginary parts leads to the following equation:

$$a_1' = -\frac{a_2^2\gamma}{4\omega_1}\left[\sin\left(\phi_2 + 2\tau_1\omega_2\right)\right] + \frac{f\sin\left(\phi_1\right)}{2\omega_1} - a_1\left[\zeta_1\omega_1 + \frac{1}{2}g_1\cos\left(\tau_4\omega_1\right)\right] \tag{12}$$

$$\begin{aligned} \theta_1' a_1 = &-\frac{a_2^2\gamma}{4\omega_1}\left[\cos\left(2\tau_1\omega_2 + \phi_2\right)\right] - \frac{f\cos\left(\phi_1\right)}{2\omega_1} \\ &+ \frac{1}{2}a_1 g_1\sin\left(\tau_4\omega_1\right) + \frac{3a_1^3\beta}{8\omega_1} + \frac{1}{4}a_1^3\delta\omega_1 \end{aligned} \tag{13}$$

$$a_2' = \frac{\alpha\omega_1 a_1 a_2}{4\omega_2}\left[\cos\left(\phi_2 + \tau_3\omega_2 - \tau_2\omega_1\right)\right] - a_2\left[\zeta_2\omega_2 - \frac{1}{2}g_2\cos\left(\tau_5\omega_2\right)\right] \tag{14}$$

$$\theta_2' a_2 = \frac{\alpha\omega_1 a_1 a_2}{4\omega_2}\left[\sin\left(\phi_2 + \tau_3\omega_2 - \tau_2\omega_1\right)\right] - \frac{1}{2}a_2 g_2\sin\left(\tau_5\omega_2\right) \tag{15}$$

where $\phi_1 = \sigma_s T_1 - \theta_1$, $\phi_2 = \theta_1 - 2\theta_2 - \sigma_c T_1$.

2.2. Equilibrium Solutions

Assuming that the amplitudes of both the cantilever beam and the controller are positive, there exist two equilibrium solutions: a single-modal solution and a coupled-modal solution, and the two modal solutions are as follows:

where $a_2 = 0$, obtain single-mode solution:

$$\begin{aligned} &a_1^2\left(\left(\frac{3\beta}{8\omega_1} + \frac{1}{4}\delta\omega_1\right)a_1^2 + \frac{1}{2}g_1\cos\left(\tau_4\omega_1\right) - \sigma_s\right)^2 \\ &+ a_1^2\left[\zeta_1\omega_1 + \frac{1}{2}g_1\sin\left(\tau_4\omega_1\right)\right]^2 = \left(\frac{f}{2\omega_1}\right)^2 \end{aligned} \tag{16}$$

where $a_2 \neq 0$, obtain coupled-mode solution:

$$a_1 = \frac{4\omega_2}{\alpha\omega_1}\sqrt{\left(\zeta_2\omega_2 - \frac{1}{2}g_2\cos\left(\tau_5\omega_2\right)\right)^2 + \left(\frac{\sigma_s - \sigma_c}{2} + \frac{1}{2}g_2\sin\left(\tau_5\omega_2\right)\right)^2} \quad (17)$$

To get the steady-state solutions of Equations (12)-(15) and to determine the stability of the equilibrium solutions, the Cartesian coordinates is introduced:

$$\begin{aligned} p_1' = &-\frac{\gamma\left(p_2^2 - q_2^2\right)\sin\left(2\tau_1\omega_2\right)}{4\omega_1} - \frac{\gamma p_2 q_2\cos\left(2\tau_1\omega_2\right)}{2\omega_1} - \zeta_1\omega_1 p_1 - q_1\sigma_s \\ &+ \frac{1}{2}g_1\left(q_1\sin\left(\tau_4\omega_1\right) - p_1\cos\left(\tau_4\omega_1\right)\right) + q_1\left(p_1^2 + q_1^2\right)\left(\frac{3\beta}{8\omega_1} + \frac{1}{4}\delta\omega_1\right) \end{aligned} \quad (18)$$

$$\begin{aligned} q_1' = &\frac{\gamma\left(p_2^2 - q_2^2\right)\cos\left(2\tau_1\omega_2\right)}{4\omega_1} - \frac{\gamma p_2 q_2\sin\left(2\tau_1\omega_2\right)}{2\omega_1} + \frac{f}{2\omega_1} + p_1\sigma_s - \zeta_1\omega_1 q_1 \\ &- \frac{1}{2}g_1\left(p_1\sin\left(\tau_4\omega_1\right) + q_1\cos\left(\tau_4\omega_1\right)\right) - p_1\left(p_1^2 + q_1^2\right)\left(\frac{3\beta}{8\omega_1} + \frac{1}{4}\delta\omega_1\right) \end{aligned} \quad (19)$$

$$\begin{aligned} p_2' = &\frac{\alpha\omega_1\left(p_1p_2 + q_1q_2\right)\cos\left(\tau_3\omega_2 - \tau_2\omega_1\right)}{4\omega_2} - \frac{q_2\left(\sigma_s - \sigma_c\right)}{2} \\ &- \frac{\alpha\omega_1\left(p_1q_2 - p_2q_1\right)\sin\left(\tau_3\omega_2 - \tau_2\omega_1\right)}{4\omega_2} - \zeta_2\omega_2 p_2 \\ &+ \frac{1}{2}g_2\left[p_2\cos\left(\tau_5\omega_2\right) - q_2\sin\left(\tau_5\omega_2\right)\right] \end{aligned} \quad (20)$$

$$\begin{aligned} q_2' = &\frac{\alpha\omega_1\left(p_2q_1 - p_1q_2\right)\cos\left(\tau_3\omega_2 - \tau_2\omega_1\right)}{4\omega_2} + \frac{p_2\left(\sigma_s - \sigma_c\right)}{2} \\ &- \frac{\alpha\omega_1\left(p_1p_2 + q_1q_2\right)\sin\left(\tau_3\omega_2 - \tau_2\omega_1\right)}{4\omega_2} - \zeta_2\omega_2 q_2 \\ &+ \frac{1}{2}g_2\left[p_2\sin\left(\tau_5\omega_2\right) + q_2\cos\left(\tau_5\omega_2\right)\right] \end{aligned} \quad (21)$$

where $p_1 = a_1\cos\left(\phi_1\right)$, $q_1 = a_1\sin\left(\phi_1\right)$, $p_2 = a_2\cos\left(\frac{\phi_1 + \phi_2}{2}\right)$, $q_2 = a_2\sin\left(\frac{\phi_1 + \phi_2}{2}\right)$.

3. Natural Frequency of a Cantilever Beam

The cantilever beam selected for the experiment is a carbon fiber beam, for which modal experiments are conducted to measure the natural frequency and vibration mode of the cantilever beam by force measurement method.

Figure 1 shows the whole experimental device is fixed on the table of the optical platform, and one end of the horizontal cantilever beam is fixed on a column clamp, which is clamped with screws, and two acceleration sensors are connected to the beam, and the sensors are general-piezoelectric sensors. The device includes a force hammer, a vibration control system, acceleration sensors, a signal acquisition and analyzer, and a PC.

The general flow of this experiment is as follows: establish a cantilever beam model in the modal module, stimulate the cantilever beam with a force hammer, collect the response signals from the acceleration sensor and the force hammer.

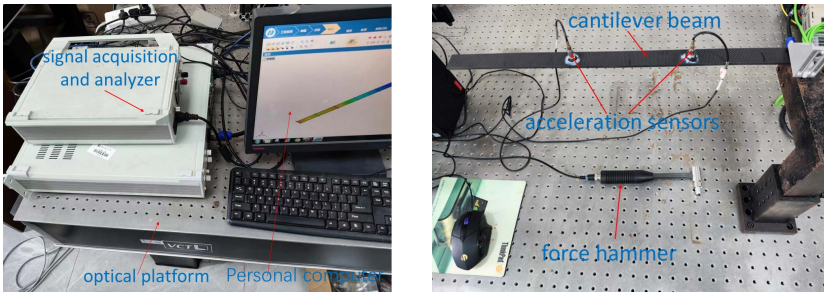

Figure 1. Experimental photos.

Figure 2 shows the mode diagram in the analysis module of the pc side, the first-order modal frequency of the cantilever beam is 16.44 Hz, which is then substituted into the subsequent calculations.

4. Effect of Parameters on Saturation Control Amplitude and Frequency Bandwidth

In order to solve for the effective saturation control damping bandwidth, and in order to further analyze the effect of the parameters on reducing the amplitude and bandwidth of the main system, it is discussed in the following two cases.

Case 1: $\sigma_c = 0$, $\omega_1 = 16.44$ Hz, $\omega_2 = \omega_1/2 = 8.22$ Hz.

Case 2: $\sigma_s = 0$, $\omega_1 = 16.44$ Hz, $\omega_2 = \omega_1/2 = 8.22$ Hz.

The equilibrium solutions can be solved by setting $p_1' = q_1' = p_2' = q_2' = 0$, the amplitude equations of the cantilever beam and the controller can be written as:

$$a_i = \sqrt{p_i^2 + q_i^2}\ (i = 1,2) \tag{22}$$

4.1. External Excitation *f* Effects on Saturation Control

The effect of external excitation on saturation control is discussed below in two cases, from **Figure 3** and **Figure 4**, it can be seen that three force sizes are chosen as $f = 0.03$, $f = 0.06$, $f = 0.09$ and other parameters are shown in **Table 1**.

Figure 3 and **Figure 4** show that with the increase of the external excitation value, the interval of saturation control continuously increases, and the response amplitude of the controller increases, in which the solid line and the hollow circle represent the stable solution and the unstable solution respectively.

Figure 4 shows that as the case 2 of the graph with internal tuning parameters changes, the amplitude of the beam does not become a straight line in the range outside the saturation control interval, and the greater the external excitation is, the larger the amplitude of the beam is. The greater the amplitude of the master system and controller within the saturated control interval.

4.2. Effects of the Nonlinear Coefficient *β*

From **Figure 5** and **Figure 6**, it can be seen that the coefficients of the cubic nonlinear coefficients are respectively $\beta = 4$, $\beta = 8$, $\beta = 12$ and $\beta = 16$, other parameters are listed in **Table 1**.

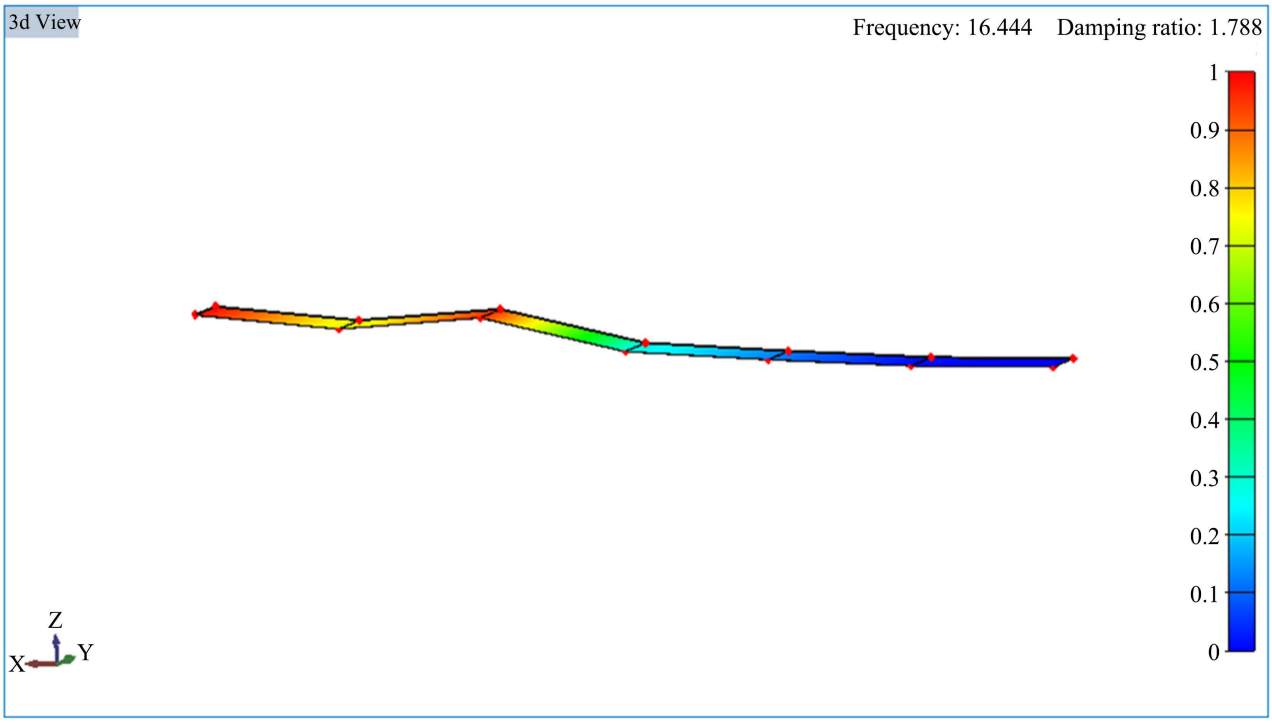

Figure 2. First order mode of vibration of the beam.

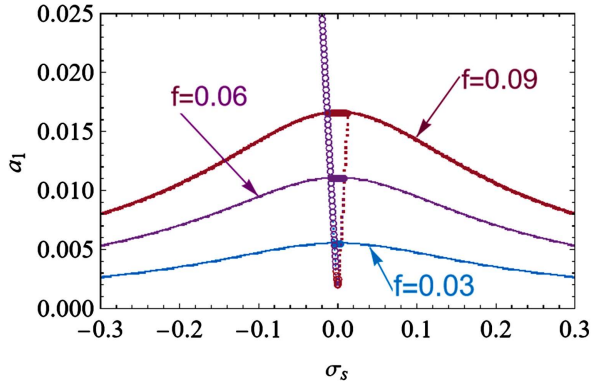

(a)

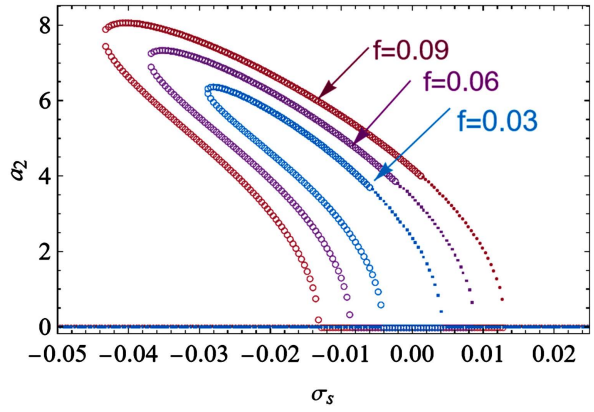

(b)

Figure 3. Amplitude-frequency response curves of Case 1: (a) beam; (b) controller.

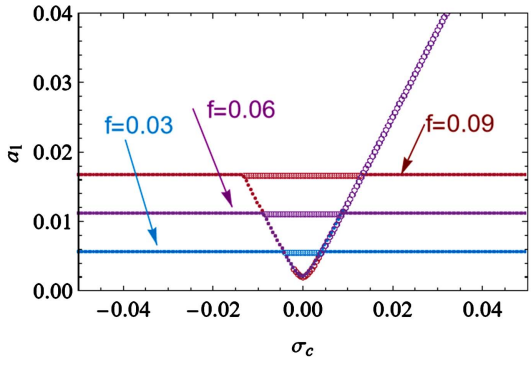

(a)

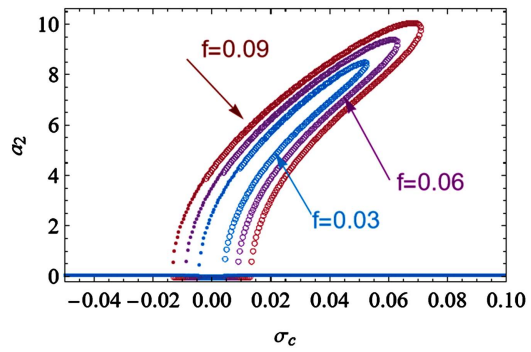

(b)

Figure 4. Amplitude-frequency response curves of Case 2: (a) beam; (b) controller.

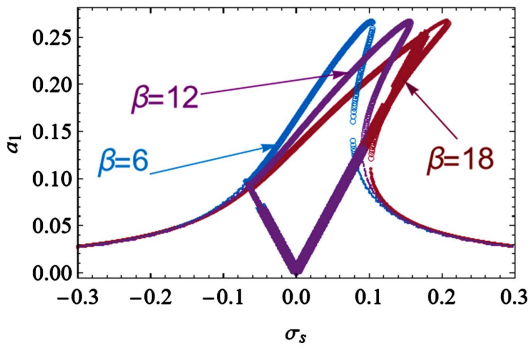

(a)

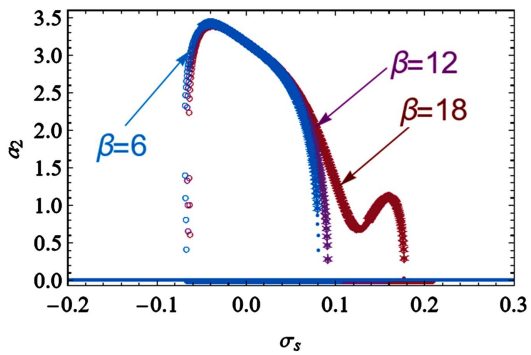

(b)

Figure 5. Amplitude-frequency response curves of Case 1: (a) beam; (b) controller.

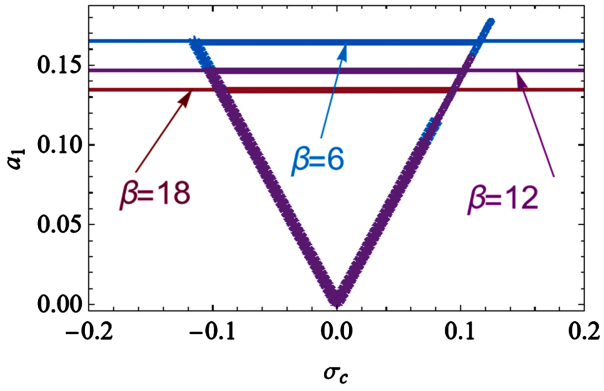

(a)

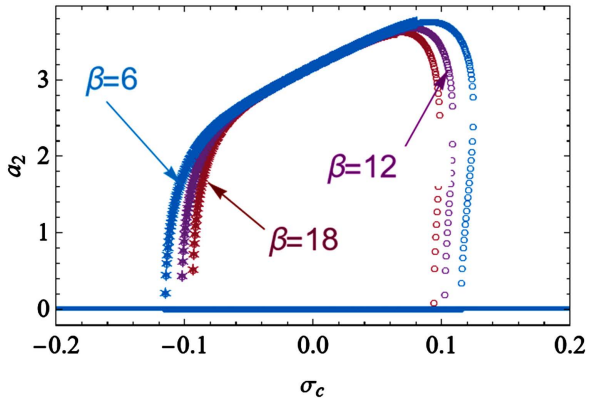

(b)

Figure 6. Amplitude-frequency response curves of Case 2: (a) beam; (b) controller.

Table 1. Physical parameters.

Physical parameters	α	β	γ
numerical value	0.8	12.21	0.01
Physical parameters	δ	ζ_1	ζ_2
numerical value	1	0.01	0.0001
Physical parameters	ω_1	ω_2	f
numerical value	16.44	8.22	0.03
Physical parameters	g_1	g_2	τ_1
numerical value	0	0	0
Physical parameters	τ_2	τ_3	
numerical value	0	0	

Figure 5 shows that as the value of the third nonlinearity coefficient increases, the saturation control interval decreases and the nonlinearity of the beam increases. The controller is stable only at positive outer tuning parameters, and has a semi-arch shape with a semi-stable region in the saturation control interval.

Figure 6 shows that when the internal tuning parameter is varied for Case 2, the main system amplitude is constant outside the saturation control interval and is a horizontal straight line that decreases with increasing values of the third nonlinear coefficient.

4.3. Feedback Coefficient g_1 Effect on Saturation Control

From Figure 7 and Figure 8 it can be seen that the selection feedback coefficients are respectively $g_1 = -0.18$, $g_1 = -0.8$, $g_1 = 0.02$ and $g_1 = 0.12$, other parameters are listed in Table 1.

Figure 7 shows that as the feedback gain coefficient decreases, the saturation control interval is increasing, the amplitude of the main system in the saturation control interval is increasing, and the amplitude of the controller is decreasing. The variation curve of the main system amplitude in the saturation control interval is axisymmetric about the outer tuning parameter and is the curve.

Figure 8 shows that unchanged amplitude of the main system outside the saturated control interval. The larger the feedback gain coefficient, the smaller the saturation control interval and the smaller the amplitude within the saturation control interval, also within the saturation control interval with respect to the internal tuning parameter $\sigma_c = 0$ axis symmetry.

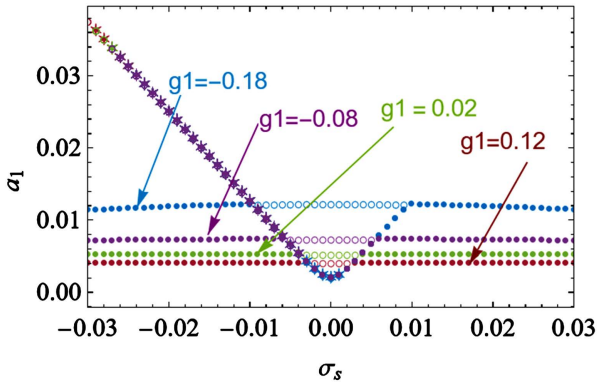

(a)

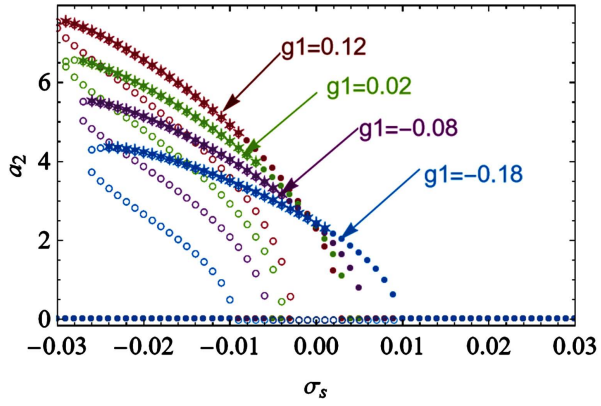

(b)

Figure 7. Amplitude-frequency response curves of Case 1: (a) beam; (b) controller.

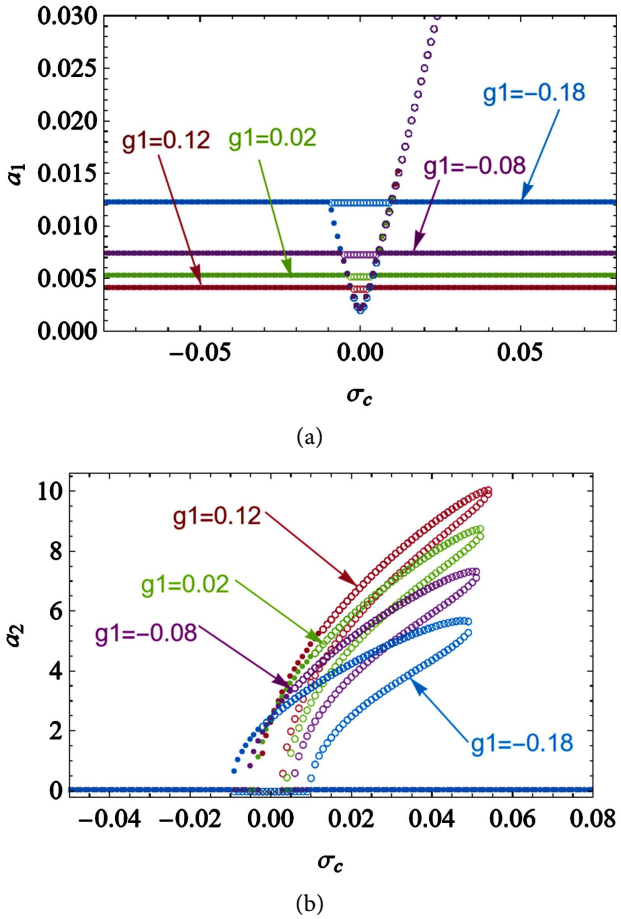

Figure 8. Amplitude-frequency response curves of Case 2: (a) beam; (b) controller.

5. Conclusions

In this paper, the effects of physical and control parameters on saturation control are investigated. The approximate solution of the vibrating system when the main resonance and the 1:2 internal resonance occur simultaneously is obtained by using the multiscale method. Through the above analysis, the following main conclusions are drawn.

The bandwidth of the saturation control can be increased by increasing the value of the external excitation, the nonlinearity of the beam is enhanced by increasing the cubic nonlinearity factor β. As the feedback gain coefficient g_1 decreases, the saturation control interval increases. Case 1 and Case 2 are the amplitude-frequency response curves of two different frequency bases; when Case 1, the variation curve of the main system amplitude in the saturation control interval is not exactly in the form of an even function, *i.e.*, it is not exactly axisymmetric with respect to the outer tuning parameter $\sigma_s = 0$; whereas, when Case 4, the variation curve of the main system amplitude in the saturation control interval is exactly axisymmetric with respect to the inner tuning parameter $\sigma_c = 0$, and the amplitude of the main system outside the saturation control interval is unchanged.

Acknowledgements

This work is supported by the National Nature and Science Foundation of China under Grant No. 12072140, Natural Science Foundation of Jiangxi Province of China under Grant No. 20202ACBL201003.

Conflicts of Interest

The authors declare no conflicts of interest regarding the publication of this paper.

References

[1] Nayfeh, A.H., Mook, D.T. and Marshall, L.R. (1973) Nonlinear Coupling of Pitch and Roll Modes in Ship Motions. *Journal of Hydronautics*, **7**, 145-152. https://doi.org/10.2514/3.62949

[2] Haddow, A.G., Barr, A.D.S. and Mook, D.T. (1984) Theoretical and Experimental Study of Modal Interaction in a Two-Degree-of-Freedom Structure. *Journal of Sound and Vibration*, **97**, 451-473. https://doi.org/10.1016/0022-460X(84)90272-4

[3] Golnaraghi, M.F. (1991) Regulation of Flexible Structures via Nonlinear Coupling. *Dynamics and Control*, **1**, 405-428. https://doi.org/10.1007/BF02169768

[4] Oueini, S.S., Nayfeh, A.H. and Pratt, J.R. (1998) A Nonlinear Vibration Absorber for Flexible Structures. *Nonlinear Dynamics*, **15**, 259-282. https://doi.org/10.1023/A:1008250524547

[5] Oueini, S.S. and Golnaraghi, M.F. (1996) Experimental Implementation of the Internal Resonance Control Strategy. *Journal of Sound and Vibration*, **191**, 377-396. https://doi.org/10.1006/jsvi.1996.0129

[6] Khajepour, A. and Golnaraghi, M.F. (1997) Experimental Control of Flexible Structures Using Nonlinear Modal Coupling: Forced and Free Vibration. *Journal of Intelligent Material Systems and Structures*, **8**, 697-710. https://doi.org/10.1177/1045389X9700800807

[7] Maccari, A. (2003) Vibration Control for the Primary Resonance of a Cantilever Beam by a Time Delay State Feedback. *Journal of Sound and Vibration*, **259**, 241-251. https://doi.org/10.1006/jsvi.2002.5144

[8] Pai, P.F., Wen, B., Naser, A.S. and Schulz, M.J. (1998) Structural Vibration Control Using PZT Patches and Non-Linear Phenomena. *Journal of Sound and Vibration*, **215**, 273-296. https://doi.org/10.1006/jsvi.1998.1612

[9] Xu, J., Chung, K.W. and Zhao, Y.Y. (2010) Delayed Saturation Controller for Vibration Suppression in a Stainless-Steel Beam. *Nonlinear Dynamics*, **62**, 177-193. https://doi.org/10.1007/s11071-010-9708-4

[10] Zhao, Y.Y. and Xu, J. (2007) Effects of Delayed Feedback Control on Nonlinear Vibration Absorber System. *Journal of Sound and Vibration*, **308**, 212-230. https://doi.org/10.1016/j.jsv.2007.07.041

[11] Zhao, Y.Y. and Xu, J. (2012) Using the Delayed Feedback Control and Saturation Control to Suppress the Vibration of the Dynamical System. *Nonlinear Dynamics*, **67**, 735-753. https://doi.org/10.1007/s11071-011-0023-5

[12] Warminski, J., Bochenski, M., Jarzyna, W., Filipek, P. and Augustyniak, M. (2011) Active Suppression of Nonlinear Composite Beam Vibrations by Selected Control Algorithms. *Communications in Nonlinear Science and Numerical Simulation*, **16**, 2237-2248. https://doi.org/10.1016/j.cnsns.2010.04.055